N-linoleyltyrosine protects PC12 cells against oxidative damage via autophagy: Possible involvement of CB1 receptor regulation

XUECHEN LIU[1*], YIYING WU[1*], DAN ZHOU[1*], YUTING XIE[1], YI ZHOU[2], YU LU[1], RUI YANG[3] and SHA LIU[1]

[1]Department of Pharmacy, Development and Regeneration Key Laboratory of Sichuan Province, Chengdu Medical College, Chengdu, Sichuan 610500; [2]Research and Development Center, Chengdu Rongsheng Pharmaceuticals Co., Ltd., Chengdu, Sichuan 610200; [3]Department of Pharmacy, Xinhua Hospital Affiliated to Shanghai Jiao Tong University School of Medicine, Shanghai 200092, P.R. China

Received March 31, 2020; Accepted July 21, 2020

DOI: 10.3892/ijmm.2020.4706

Abstract. Oxidative stress is one of the main pathogenic factors of neurodegenerative diseases. As the ligand of cannabinoid type 1 (CB1) and 2 (CB2) receptors, anandamide (AEA) exerts benign antioxidant activities. However, the instability of AEA results in low levels *in vivo*, which limit its further application. Based on the structure of AEA, N-linoleyltyrosine (NITyr) was synthesized in our laboratory and was hypothesized to possess a similar function to that of AEA. To the best of our knowledge, the present study demonstrates for the first time, the activities and mechanisms of NITyr. NITyr treatment attenuated hydrogen peroxide (H_2O_2)-induced cytotoxicity, with the most promiment effect observed at 1 μmol/l. Treatment with NITyr also suppressed the H_2O_2-induced elevation of reactive oxygen species (ROS) and enhanced the expression of the autophagy-related proteins, LC3-II, beclin-1, ATG 5 and ATG13. The autophagic inhibitor, 3-methyladenine, reversed the effects of NITyr on ROS levels and cellular viability. Furthermore, AM251, a CB1 receptor antagonist, but not AM630 (a CB2 receptor antagonist), diminished the effects of NITyr on cell viability, ROS generation and autophagy-related protein expression. However, NITyr increased the protein expression of both the CB1 and CB2 receptors. Therefore, NITyr was concluded to protect PC12 cells against H_2O_2-induced oxidative injury by inducing autophagy, a process which may involve the CB1 receptor.

Correspondence to: Professor Sha Liu, Department of Pharmacy, Development and Regeneration Key Laboratory of Sichuan Province, Chengdu Medical College, 783 Xindu Avenue, Chengdu, Sichuan 610500, P.R. China
E-mail: liushamaliang@163.com

Dr Rui Yang, Department of Pharmacy, Xinhua Hospital Affiliated to Shanghai Jiao Tong University School of Medicine, 1665 Kongjiang Road, Shanghai 200092, P.R. China
E-mail: yangr.2007@163.com

*Contributed equally

Key words: N-linoleyltyrosine, cannabinoid receptor, autophagy, oxidative stress, PC12 cells

Introduction

Oxidative stress refers to the increase in free radicals or the weakening of the body's antioxidant protective ability following stimulation with harmful factors, leading to an imbalance in the oxidation and antioxidant systems (1). The excessive accumulation of reactive oxygen species (ROS) damages biological molecules, such as nucleic acids, proteins and lipids, resulting in the occurrence and development of cardiovascular diseases, Alzheimer's disease and other chronic degenerative diseases. Antioxidants can alleviate or inhibit cellular damage by neutralizing free radicals (2,3).

Autophagy is a process through which the body removes aged, damaged or defective proteins and organelles. During autophagy, the degradable contents of the cytoplasm are encapsulated in subcellular bilayer vesicles and then transported to lysosomes for degradation (4). Recent studies have suggested that autophagy exerts protective effects against neurodegeneration, in which autophagic deficiency was associated with a decline in learning and memory (5). The importance of autophagy in the reduction of oxidative stress has also been recognized, and several autophagy inducers have been tested for their therapeutic potential (6). Previous studies have indicated that the autophagic flux is inhibited under conditions of oxidative stress in degenerative diseases (6,7); thus, it was hypothesized that the induction of autophagy may be a promising antioxidant approach.

It has been demonstrated that as the ligand for the cannabinoid type 1 (CB1) and 2 (CB2) receptors, anandamide (AEA) exerts neuroprotective effects by inhibiting oxidative stress and free radical formation (8). Additionally, cannabinoids and activating cannabinoid receptors induce autophagy in cardiovascular disease (9-11). However, the rapid metabolic inactivation of AEA *in vivo* has limited its further application (12); thus, the development of novel AEA analogs is of

considerable importance. Based on the chemical structure of AEA (Fig. 1), its analogue, N-linoleyl tyrosine (NITyr), was previously synthesized in our laboratory (13). To the best of our knowledge, the present study aimed to demonstrate for the first time, the effects and potential mechanisms of NITyr on autophagy in rat pheochromocytoma (PC12) cells under conditions of oxidative stress.

Materials and methods

Materials. NITyr was previously independently synthesized (13). The following additional reagents were used in the present study: Polyclonal antibodies against LC3, beclin-1, autophagy-related protein (ATG) 5 and the CB1 receptor (1:1,000, cat. nos. 14600-1-AP, 11306-1-AP, 10181-2-AP and 17978-1-AP, respectively; ProteinTech Group, Inc.); CB2 receptor rabbit polyclonal antibody (1:500; cat. no. 101550, Cayman Chemical Company); ATG13 rabbit polyclonal antibody (1:1,000; cat. no. 500690, Chengdu Zen Bioscience Co., Ltd.); GAPDH rabbit polyclonal antibody (1:2,000; cat. no. 60004-1-AP, ProteinTech Group, Inc.); horseradish peroxidase (HRP)-conjugated goat anti-mouse/anti-rabbit IgG(H+L) (1:10,000; cat. no. AB0102, cat. no. AB0101, Abways Technology, Inc.); Alexa Fluor 594-conjugated goat anti-rabbit IgG (H+L) (1:500; cat. no. AB0141, Abways Technology, Inc.); CB1 receptor antagonist AM251 (cat. no. S2819, Selleck Chemicals); CB2 receptor antagonist AM630 (cat. no. SML0327, Sigma-Aldrich, Merck KGaA); 3-methyladenine (3MA; cat. no. 19389, CSNpharm, Inc.); hydrogen peroxide (H_2O_2; cat. no. 20180610, Chengdu Jinshan Chemical Reagent Co., Ltd.); and Dulbecco's modified Eagle's medium (DMEM; cat. no. SH30809, HyClone; Cytiva).

Cell culture and experimental groupings. PC12 cells were cultured in DMEM supplemented with 10% fetal calf serum, 5,000 U/ml penicillin and 5 mg/ml streptomycin. The cells were cultured at 37˚C in an incubator supplemented with 5% CO_2, and sub-cultured every 2 days. Subsequently, the cells were seeded and pre-incubated with combinations of NITyr (0.5, 1 or 5 μmol/l), 3MA (3 mmol/l), AM251 (3 μmol/l) and AM630 (3 μmol/l) for 24 h. This was followed by the addition of 250 μmol/l H_2O_2 and the cells were incubated for a further 24 h. Following the drug treatments, the cells were stained with 3-(4,5-dimethylthiazol-2-yl)-2,5-diphenyltetrazodium bromide (MTT), 4',6-diamidino-2-phenylindole (DAPI) or 2',7-dichlorofluorescin diacetate (DCFH-DA), and western blot analysis and immunofluorescence evaluation were performed. The experimental groups were as follows: i) Control; ii) 50, 100, 250 or 500 μmol/l H_2O_2; iii) H_2O_2+ 0.5, 1 or 5 μmol/l NITyr, respectively; iv) H_2O_2 + 1 μmol/l NITyr and 3 μmol/l AM251; v) H_2O_2 + 1 μmol/l NITyr and 3 μmol/l AM630; vi) H_2O_2 + 3 μmol/l AM251; and vii) H_2O_2 + 3 μmol/l AM630; viii) control + 5 μmol/L NITyr. The concentrations of AM251 and AM630 were determined according to the published literature and previous experimental findings (14,15).

Cell viability assay. PC12 cells were seeded into 96-well plates at a density of $5x10^4$ cells/100 μl, and cultured in an incubator at 37˚C (5% CO_2) for 24 h. The cells were then treated with various concentrations of H_2O_2 (50, 100, 250 and 500 μmol/l) and NITyr (0.5, 1 and 5 μmol/l) for 12, 24 and 48 h, respectively. Subsequently, 10 μl MTT solution (5 mg/ml) were added to each well and the plates were incubated for a further 4 h at 37˚C. The formamide was dissolved using dimethyl sulfoxide (100 μl/well), and the absorbance of each sample was detected at 560 nm using a VICTOR Nivo™ multimode plate reader (PerkinElmer, Inc.).

DAPI and DCFH-DA staining. Intracellular DNA damage and ROS generation were assessed using DAPI (1:1,000; Beyotime Institute of Biotechnology) and DCFH-DA probes (1:1,000; Dalian Meilun Biology Technology Co., Ltd.), respectively. Following drug treatment, PC12 cells (at a density of $2.5x10^5$ cells/well) were incubated in serum-free DMEM containing DAPI at room temperature for 10 min, or DCFH-DA at 37˚C for 20 min. The 6-well plate was then rinsed 3 times in PBS (5 min each) and immediately analyzed using a fluorescence microscope (magnification x20 and x40; Olympus Corporation). The relative fluorescence intensity of DCFH-DA was analyzed using a fluorometer (Thermo Fisher Scientific, Inc.).

Immunofluorescence assay. PC12 cells were seeded onto coverslips at a density of $25x10^4$ cells/well and placed into 6-well plates. Following drug treatment, the cells were treated according to a previously described immunofluorescence protocol (16). The coverslips were rinsed 3 times with PBS for 5 min each time, immobilized with 4% paraformaldehyde for 15 min and permeabilized with 0.5% Triton X-100 for 20 min in room temperature. The cells were rinsed again and blocked with 5% bovine serum albumin (BSA) for 1 h at room temperature. Each coverslip was then incubated with the corresponding primary antibodies (LC3, beclin-1, ATG5, ATG13, CB1 and CB2) diluted in Tris-buffered saline with Tween-20 (TBST) (1% BSA) overnight at 4˚C, and subsequently washed with 1X TBST (3 times for 3 min each) prior to incubation with an Alexa Fluor 594-conjugated secondary antibody for 1 h at room temperature in the dark. Subsequently, 1 μg/ml DAPI was added to detect the cell nuclei, and the cells were finally washed 5 times with 1X TBST for 8 min each time and observed using a BX63 fluorescence microscope (magnification x20 and x40; Olympus Corporation).

Western blot analysis. PC12 cells were seeded at a density of $1x10^6$ cells/well and cultured in 6-well plates for 24 h. Following drug treatment, the cells were treated according to the following western blotting protocol: The cells were washed 3 times with PBS for 5 min each time, and then incubated on ice for 30 min in prepared lysis buffer (RIPA lysis buffer, protease inhibitor and EDTA at a 100:1:1 ratio; all Beyotime Institute of Biotechnology, Inc.). Following lysis, the cells were centrifuged at 12,000 x g for 20 min at 4˚C, and the supernatants were collected. The protein concentration was then detected and adjusted according to the instructions of the Easy II Protein Quantitative Kit (BCA, TransGen Biotech Co., Ltd.), and the samples were then denatured at 100˚C for 6 min. To detect proteins with different molecular weights, 50 μg protein per lane were separated using 10% polyacrylamide gels (Tris-HCl system), and then transferred onto polyvinylidene difluoride membranes (Merck Millipore Ltd.). The

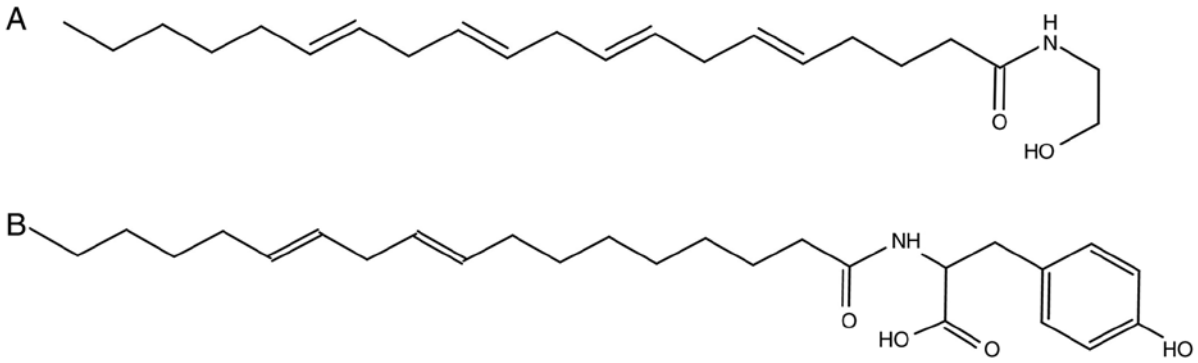

Figure 1. Chemical structure of (A) AEA and (B) NITyr. AEA, anandamide; NITyr, N-linoleyltyrosine.

membranes were blocked with 5% BSA on a shaking platform at 37˚C for 1 h, and then incubated with the corresponding primary antibodies (LC3, beclin-1, ATG5, ATG13, CB1 and CB2) overnight at 4˚C; a GAPDH rabbit polyclonal antibody was used to detect the internal control. Subsequently, the membranes were washed with TBST 3 times for 5 min each, and then incubated with secondary HRP-conjugated antibodies at room temperature for 1 h. Finally, the membranes were washed with TBST as aforementioned, and treated with chemiluminescent HRP substrate (EMD Millipore) for protein band detection. Images were captured using a ChemiDoc system (Bio-Rad Laboratories, Inc.), and the gray values of the proteins were quantified using Image J software 1.8.0 (NIH) with GAPDH as the comparative internal control.

Statistical analyses. SPSS statistical software 17.0 (SPSS, Inc.) was used for statistical experimental analysis and all data are expressed as the means ± standard deviation. For comparisons between groups, the data were evaluated by one-way ANOVA followed by Tukey's test. $P<0.05$ was considered to indicate a statistically significant difference.

Results

NITyr protects PC12 cells against H_2O_2 insults. Following exposure to H_2O_2, cell viability was assessed by MTT assay and was shown to be significantly decreased in a time- and concentration-dependent manner. The cell survival rates decreased gradually as a result of exposure to 100, 250 and 500 μmol/l H_2O_2, respectively ($P<0.05$ and $P<0.001$, respectively; Fig. 2A). Ultimately, the concentration of 250 μmol/l H_2O_2 was selected to induce cellular damage, as this induced a plateau in the cell viability results, and 500 μmol/l induced further cellular damage without an obvious difference in viability. Following exposure to 250 μmol/l H_2O_2, the cell survival rates decreased gradually at the 12, 24 and 48 h time points, respectively (Fig. 2B). As exposure to H_2O_2 for 48 h resulted in considerable cellular injury, the following experiments were conducted with 250 μmol/l H_2O_2 for 24 h. Additionally, the numbers of the nuclei in the H_2O_2-treated group were decreased compared with those in the control group (Fig. 2C and D). However, treatment with NITyr (0.5, 1 and 5 μmol/l) conferred a benign effect against H_2O_2-induced injury, with optimal recovery occurring at the concentration of 1 μmol/l NITyr ($F=14.841$, $P<0.05$ and $P<0.01$; Fig. 2E), and NITyr alone did not affect cellular viability compared with the control group. In addition, the results of DAPI staining indicated that detrimental changes in cellular morphology were prevented by various concentrations of NITyr (Fig. 2D), which was consistent with the results of MTT.

NITyr inhibits ROS-mediated H_2O_2-induced cellular injury. Considering the importance of ROS in H_2O_2-induced cytotoxicity, the levels of ROS in PC12 cells were evaluated following pre-treatment with 0.5, 1 or 5 μmol/l NITyr. As shown in Fig. 3A, an increased number of green dots (representing DCFH-DA fluorescence) was observed in the PC12 cells exposed to H_2O_2 compared with the control cells. NITyr effectively decreased the number of green dots induced by H_2O_2, indicating a reduction in ROS production. Furthermore, the relative fluorescence intensity of DCFH-DA was detected by fluorometry, and the elevation in H_2O_2-induced fluorescence was inhibited in the NITyr group (0.5, 1 and 5 μmol/l) with optimal rescue occurring at 1 μmol/l ($F=16.052$, $P<0.01$ and $P<0.05$; Fig. 3B); thus, the concentration of 1 μmol/l NITyr was used in the following experiments to investigate the underlying mechanisms of NITyr.

3MA attenuates the effects of NITyr on cell viability and ROS levels. As shown in Fig. 4A, pre-treatment with 3MA following H_2O_2 exposure had no significant effect on the number of cell nuclei or ROS levels compared with H_2O_2 exposure, and the DCFH-DA fluorescence intensity of the 3MA group approached that of the H_2O_2 group. 3MA combined with NITyr exerted a weaker effect on cell viability and ROS levels than treatment with 1 μmol/l NITyr following H_2O_2 exposure. Moreover, the relative DCFH-DA fluorescence intensity and cell viability were detected by fluorometry and MTT assay, respectively. The results were consistent with those of DCFH-DA and DAPI staining ($F=15.704$, $F=27.591$, $P<0.05$; Fig. 4B and C).

Effects of NITyr on the expression of autophagy-related proteins. As shown in Fig. 5, compared with the control group, cell numbers in the H_2O_2 group were notably decreased (as indicated by the decreased level of blue fluorescence) and shriveling of the nuclei was apparent. Reduced levels of red fluorescence indicate decreased protein expression of LC3, beclin-1, ATG5 and ATG13, which was reversed by treatment with NITyr.

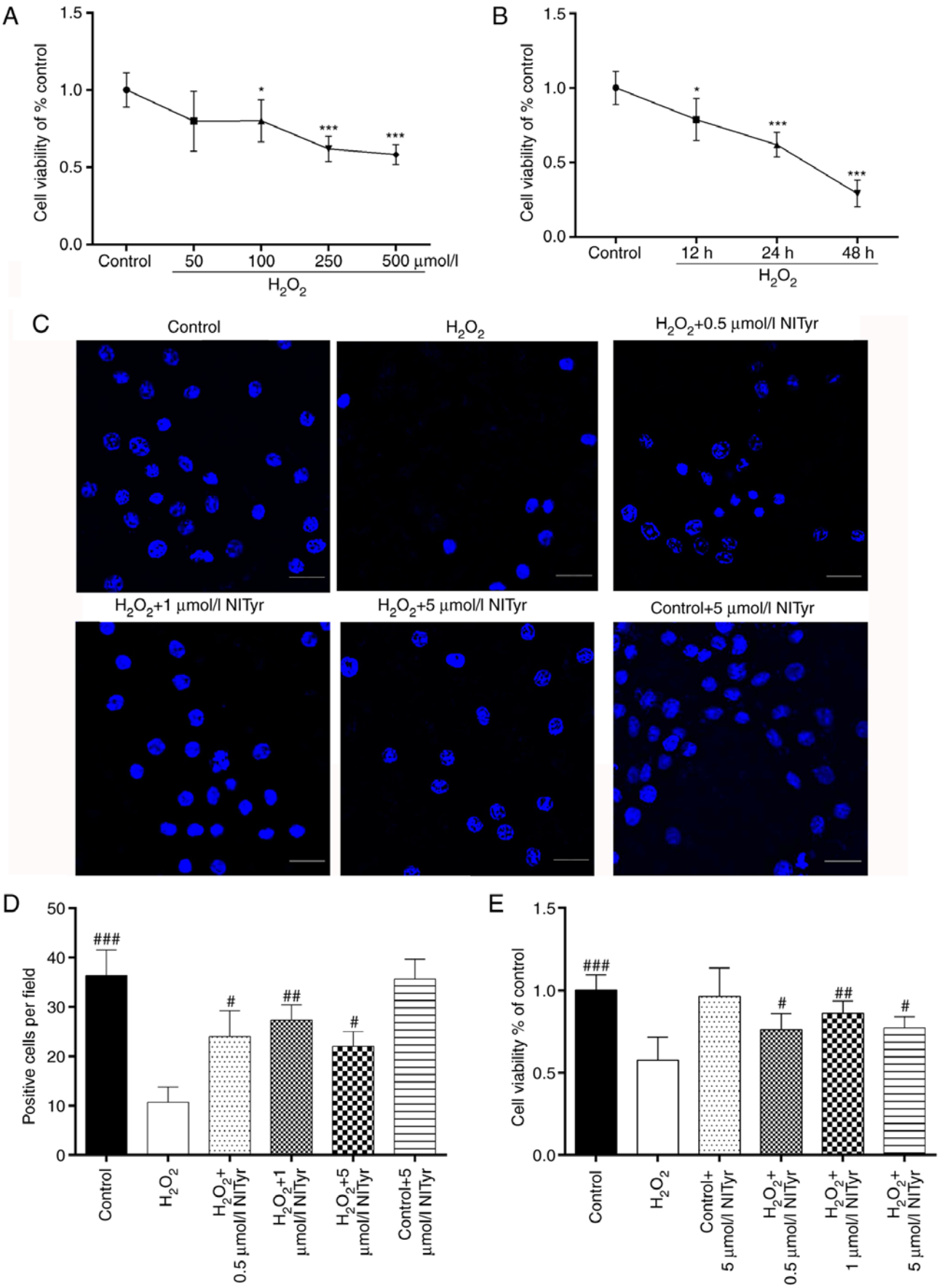

Figure 2. Effects of NITyr on PC12 cell viability. (A) Cellular injury induced by treatment with 50, 100, 250 and 500 μmol/l H_2O_2 for 24 h. (B) Cellular injury induced by 250 μmol/l H_2O_2 at different time points (12, 24 and 48 h). (C) Cell nuclei were stained using DAPI and visualized by fluorescence microscopy. Scale bar, 20 μm. (D) Quantification of the number of nuclei in PC12 cells. (E) PC12 cells were pre-treated with or without NITyr (0.5, 1 or 5 μmol/l) for 24 h prior to 250 μmol/l H_2O_2 exposure, and viability was assessed by MTT assay. Statistical values are expressed as the mean ± SD from 6 independent experiments. *P<0.05 and ***P<0.001 vs. the control group; $^{\#}$P<0.05, $^{\#\#}$P<0.01 and $^{\#\#\#}$P<0.001 vs. the H_2O_2 group. NITyr, N-linoleyltyrosine; H_2O_2, hydrogen peroxide.

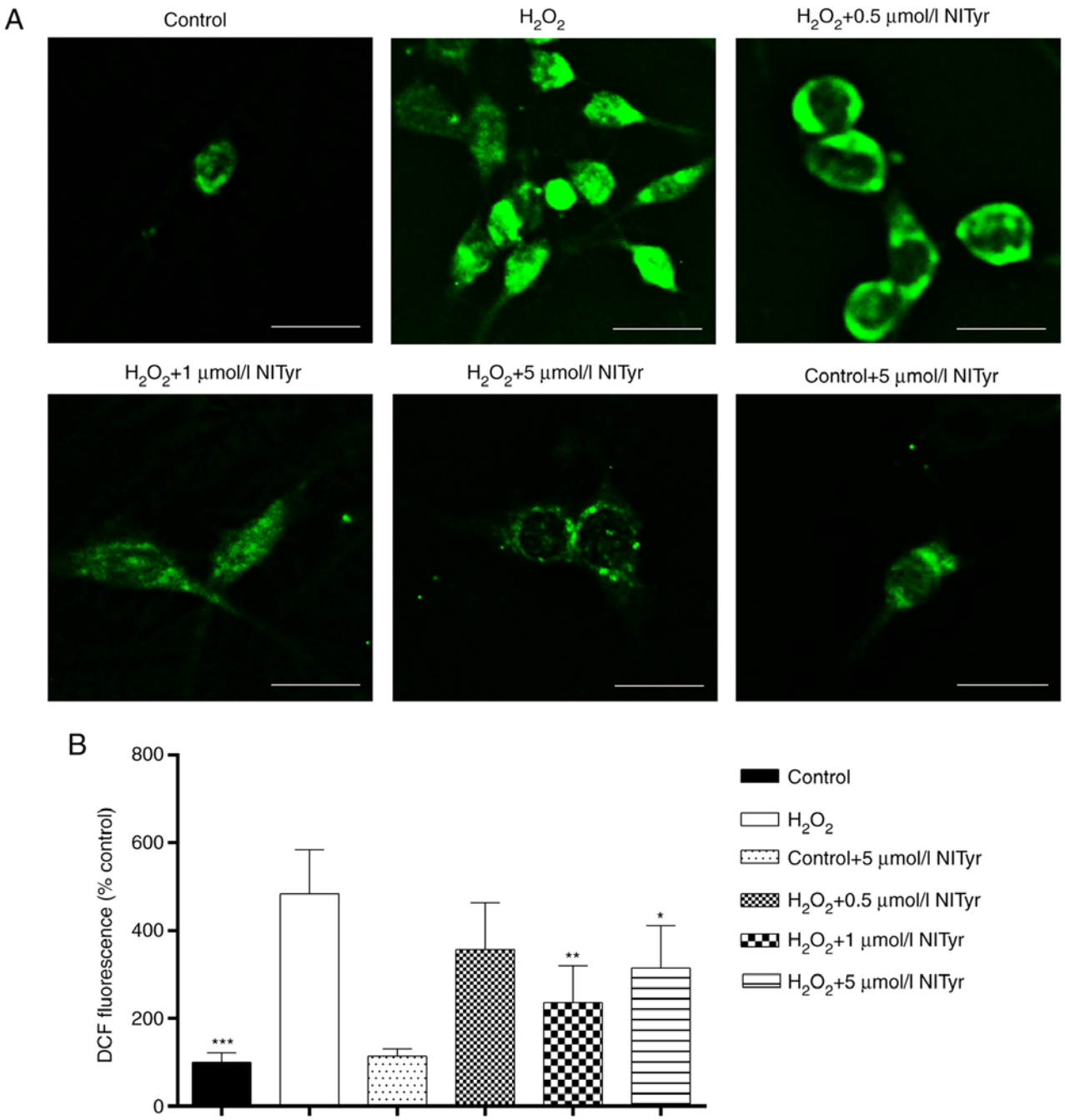

Figure 3. NITyr reduces H_2O_2-induced ROS generation. (A) Levels of ROS were detected by fluorescence microscopy with DCFH-DA as the fluorescent probe. Scale bar, 20 μm. (B) Relative DCFH-DA fluorescence intensity was detected using a fluorometer. Statistical values are expressed as the mean ± SD from 6 independent experiments. *P<0.05, **P<0.01 and ***P<0.001 vs. the H_2O_2 group. NITyr, N-linoleyltyrosine; H_2O_2, hydrogen peroxide; ROS, reactive oxygen species; DCFH-DA, 2',7-dichlorofluorescin diacetate.

Effects of CB receptor antagonists on cell viability and ROS production. Compared with H_2O_2 exposure, pre-treatment with the CB1 receptor antagonist, AM251, or the CB2 antagonist, AM630, following H_2O_2 exposure had negligible effects on cell viability and ROS levels (Fig. 6A and C). However, AM251, but not AM630, diminished the effects of NITyr (1 μmol/l) on cell viability and ROS generation. Moreover, the relative DCFH-DA fluorescence intensity and cell viability were detected by fluorometry and MTT assay, respectively, and the results were consistent with those of DCFH-DA and DAPI staining ($F_{(DCFH-DA)}$=11.502, $F_{(DAPI)}$=14.973, P<0.05; Fig. 6B and D).

Effects of the CB1 receptor antagonist, AM251, on autophagy-related proteins. According to the aforementioned experimental results, the PC12 cells were treated with a combination of 1 μmol/l NITyr and 3 μmol/l AM251. Compared with the H_2O_2 group, negligible effects on the protein expression of LC3-II, ATG5 and ATG13 (P>0.05), but significant effects on beclin-1 protein expression (P<0.05) were observed in the AM251 group following H_2O_2 exposure (Fig. 7A and C-F). When used in combination with AM251, 1 μmol/l NITyr exerted diminished effects on autophagy-related protein expression than when used alone ($F_{(LC3-II)}$=5.786, $F_{(Beclin-1)}$=533.174, $F_{(ATG-5)}$=15.479, $F_{(ATG-13)}$=11.639, P<0.05; Fig. 7A and C-F). In

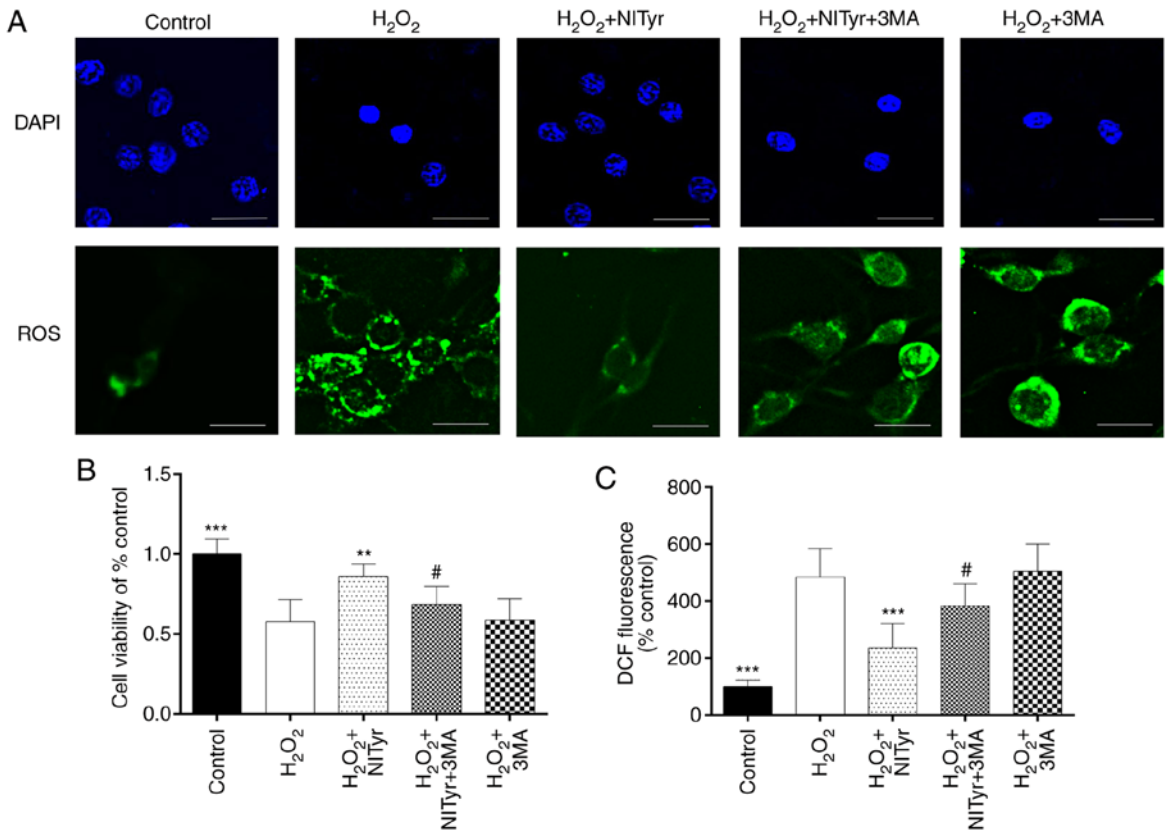

Figure 4. Effects of NITyr and 3MA on cell viability and ROS generation. (A) Nuclei were stained with DAPI and visualized by fluorescence microscopy. Levels of ROS were detected by fluorescence microscopy with DCFH-DA as the fluorescent probe. Scale bar, 20 μm. (B) Cell viability was assessed using an MTT assay. (C) Relative DCFH-DA fluorescence intensity was detected with a fluorometer. Statistical values are expressed as the means ± SD from 6 independent experiments. **P<0.01 and ***P<0.001 vs. the H_2O_2 group. $^{\#}$P<0.05 vs. the H_2O_2 + NITyr group. NITyr, N-linoleyl tyrosine; 3MA, 3-methyladenine; H_2O_2, hydrogen peroxide; ROS, reactive oxygen species; DCFH-DA, 2',7-dichlorofluorescin diacetate.

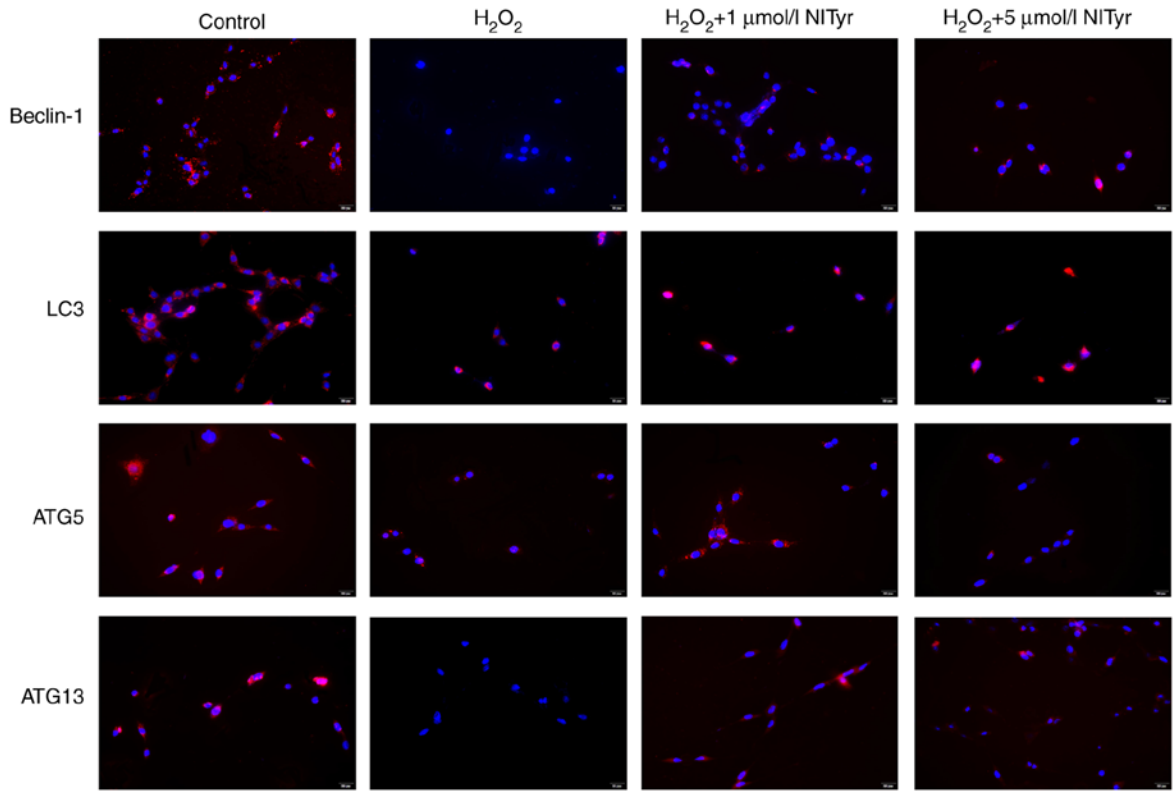

Figure 5. Effects of NITyr on the expression of autophagy-related proteins. The protein expression levels of beclin-1, LC3, ATG5 and ATG13 were detected using immunofluorescence staining. Scale bar, 50 μm. NITyr, N-linoleyltyrosine; ATG, autophagy-related protein.

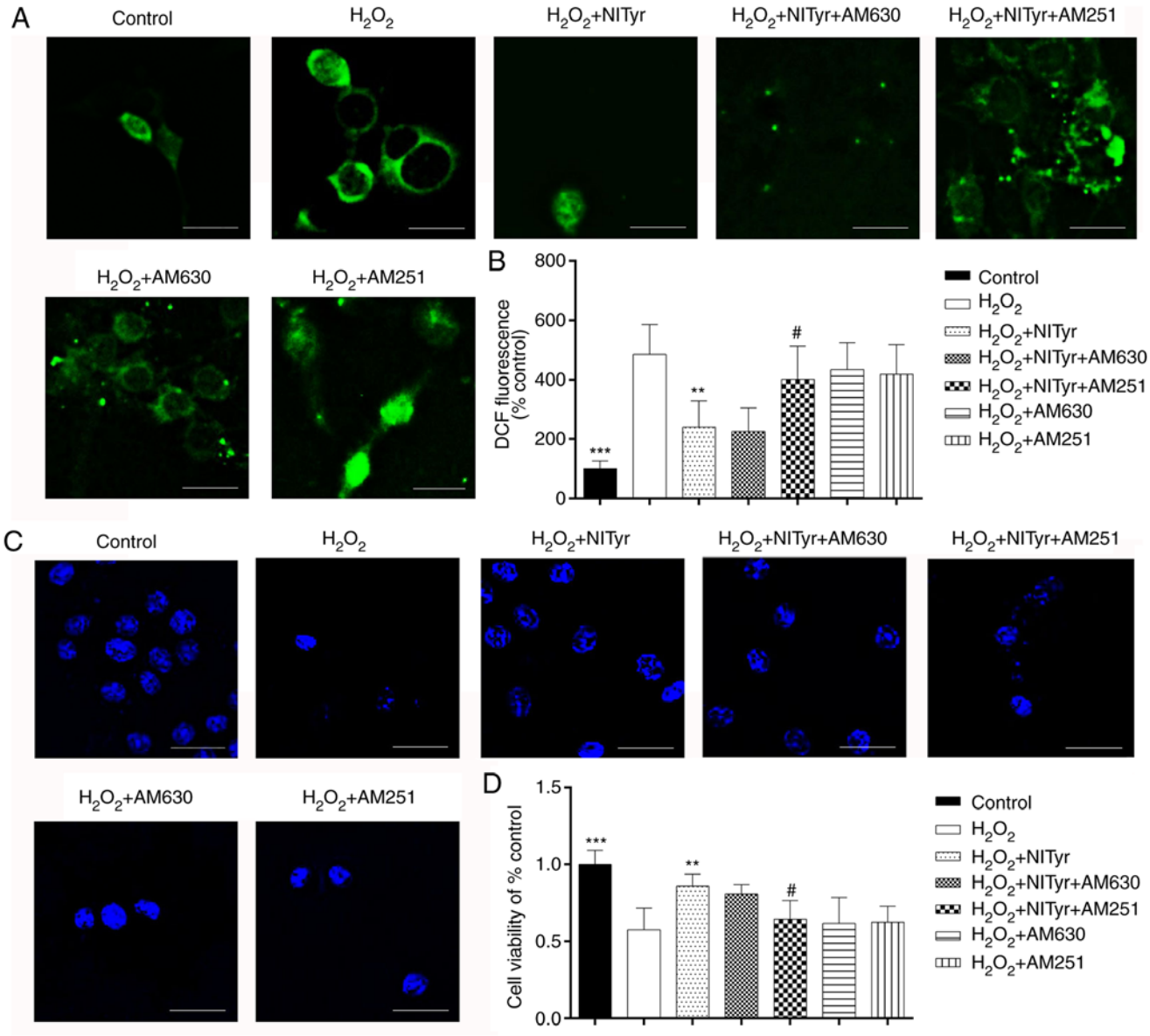

Figure 6. Effects of NITyr, AM251 and AM630 on cell viability and ROS levels. (A) Levels of ROS were detected by fluorescence microscopy with DCFH-DA as the fluorescent probe. Scale bar, 20 μm. (B) Relative DCFH-DA fluorescence intensity was detected using a fluorometer. (C) Nuclei were stained with DAPI and visualized by fluorescence microscopy. Scale bar, 20 μm. (D) Cell viability was assessed by MTT assay. Statistical values are expressed as the means ± SD from 6 independent experiments. **P<0.01 and ***P<0.001 vs. the H_2O_2 group. $^{\#}$P<0.05 vs. the H_2O_2 + NITyr group. NITyr, N-linoleyltyrosine; ROS, reactive oxygen species; DCFH-DA, 2',7-dichlorofluorescin diacetate; H_2O_2, hydrogen peroxide.

addition, compared with the control group, negligible effects of NITyr were observed on the protein expression of LC3-II, Beclin-1, ATG5 and ATG13 (P>0.05; Fig. 7B, G and H).

Effects of NITyr on CB1 and CB2 receptor expression. Significant effects on CB1 and CB2 protein expression were observed in the H_2O_2 + NITyr group compared with the H_2O_2 group (P<0.05; Fig. 8A, C and D). In addition, negligible effects were observed on the protein expression of CB1 and CB2 in the control + NITyr group compared with the control group (P>0.05). As shown in Fig. 8B, red fluorescence represents the protein expression of the CB1 and CB2 receptors. Compared with the control group, CB1, but not CB2 receptor expression levels were downregulated in the H_2O_2 group. Furthermore, pre-treatment with 1 μmol/l NITyr increased the intensity of red fluorescence compared with H_2O_2 exposure alone.

Discussion

AEA has been shown to exert benign antioxidant activity, but its short half-life is a limitation to its clinical application (8,17). In previous studies, the saturated fatty acyl amino acid, NSTyr, was synthesized based on the structure of AEA, and this compound was found to possess strong antioxidant properties (18-20). However, NSTyr must be used at a considerably higher concentration than AEA to elicit a moderate antioxidant effect (21). Based on the level of activity, the structure of AEA was compared with that of NSTyr, and AEA was found to possess unsaturated bonds, while NSTyr did not. The method for NSTyr synthesis was subsequently improved to include the incorporation of unsaturated bonds. Due to the strong antioxidant activities of AEA and NSTyr, it was speculated that NITyr also possessed antioxidant properties. Therefore,

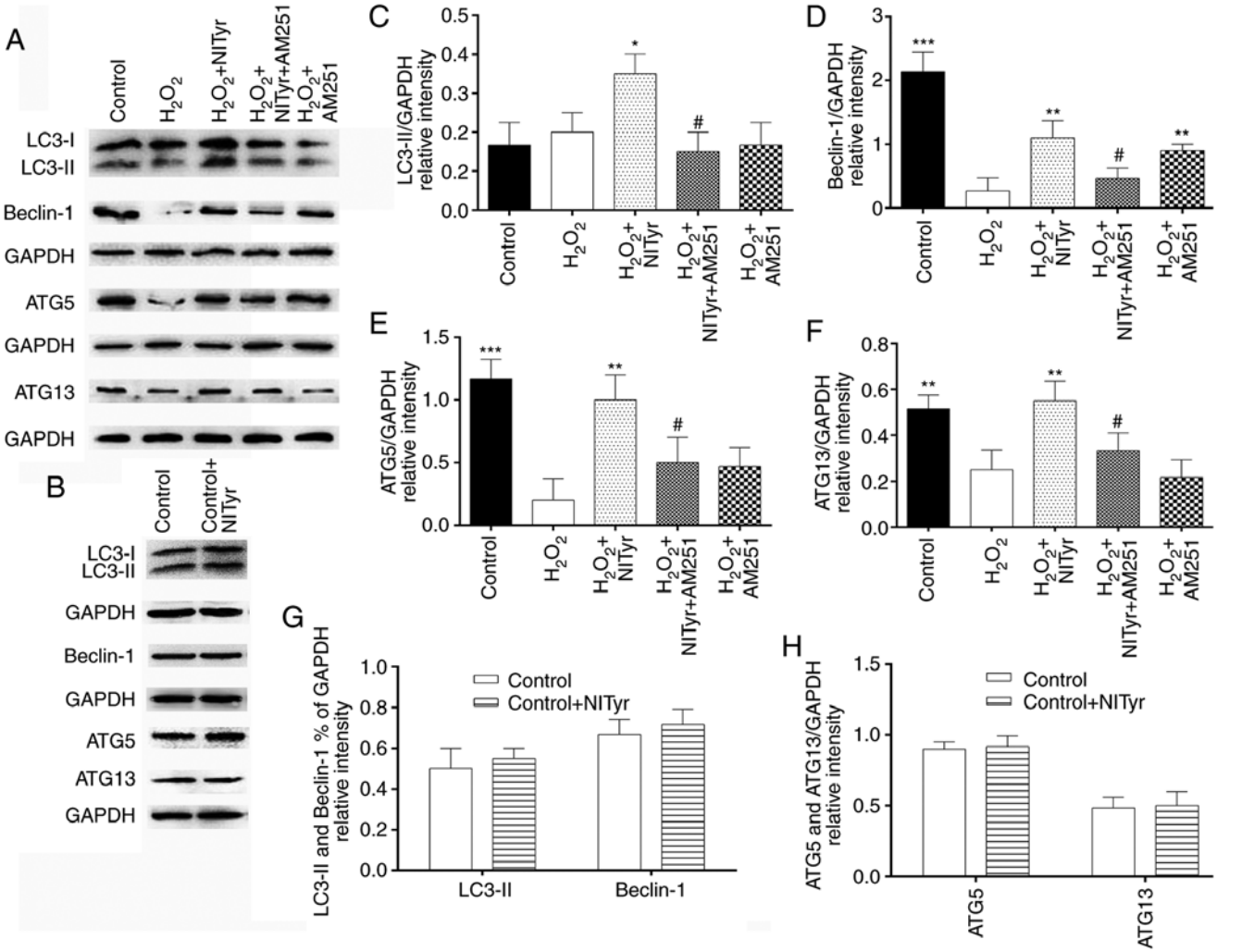

Figure 7. Effects of NITyr and AM251 on the expression of autophagy-related proteins. (A and B) Protein expression levels of LC3, beclin-1, ATG5 and ATG13 were determined by western blot analysis. (C) LC3-II, (D) Beclin-1, (E) ATG5 and (F) ATG13 expression was normalized to that of GAPDH. (G) LC3-II and Beclin-1 expression were normalized that of GAPDH. (H) ATG5 and ATG13 expression levels were normalized to those of GAPDH. Statistical values are expressed as the means ± SD from 3 independent experiments. *P<0.05, **P<0.01 and ***P<0.001 vs. the H_2O_2 group. $^{\#}$P<0.05 vs. the H_2O_2 + NITyr group. NITyr, N-linoleyltyrosine; ATG, autophagy-related protein.

the aim of the present study was to determine the potential antioxidant effects of NITyr, and the underlying mechanisms through which these effects are elicited.

Due to a high demand for oxygen in brain tissue, the central nervous system is particularly vulnerable to hypoxia, and cell membranes are prone to attack by oxygen free radicals. In general, oxidative stress has been confirmed to be elevated in neurodegenerative diseases (22,23). There is also increasing evidence that excessive intracellular H_2O_2 is toxic to the cell membrane and contributes to oxidative stress through virous ways, such as formation of reactive oxygen species, etc. Therefore, in the present study, PC12 cells were stimulated with H_2O_2 to establish an oxidative damage model (23). The fact that oxidative stress activates contradictory signaling pathways of survival and death implies that there must be sophisticated crosstalk between these opposite signals that dictate cells fate. A number of Akt substrates have been identified as elements of the initiation and execution phases of apoptosis. Akt appears to be a substrate of caspase-3 *in vitro*. So Akt signaling pathway is not only related to cell survival, but also to cell apoptosis (24,25). Combined with the literature, it is hypothesized that under the early stimulation of low concentration of H_2O_2, cells will activate their own defense mechanism to resist damage via AKT activation, resulting in cells proliferation. However, under the long stimulation of high concentration of H_2O_2, the defense mechanism initiated by cells is not sufficient to resist the injury; thus, cell viability is reduced. Therefore, the activation of the Akt pathway induced by H_2O_2 leads to cell proliferation or cell death, which may be related the concentration and time of H_2O_2 stimulation (26). In a previous study, NITyr activated the Akt signaling pathway to delay cell injury in the ischemia-reperfusion model (13). NITyr was demonstrated to markedly suppress H_2O_2-induced cellular damage and ROS generation, and this protective effect was amplified with NITyr treatement. The optimum concentration of NITyr was 1 μmol/l, and a plateau effect was reached at 5 μmol/l. Collectively, the results of the present study indicate that H_2O_2 promotes cellular injury, and that NITyr inhibits ROS-induced damage resulting from H_2O_2 exposure.

Autophagy is a highly conserved catabolic process for the removal of damaged organelles that can result in the production of intracellular ROS (27). The presence of excess ROS

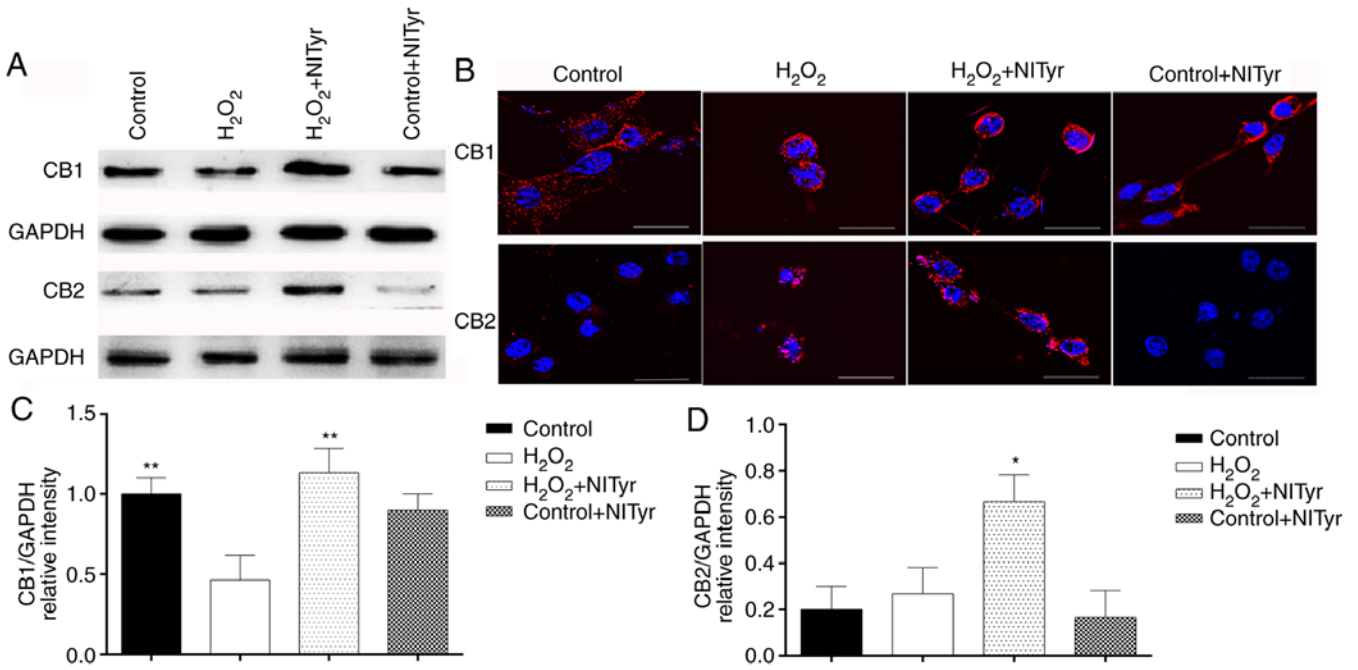

Figure 8. Effects of NITyr on the protein expression of the CB1 and CB2 receptors. (A) Protein expression levels of CB1 and CB2 were determined by western blot analysis. (B) CB1 and CB2 receptor protein expression were detected using immunofluorescence staining. (C) CB1 expression was normalized that of GAPDH. (D) CB2 expression was normalized that of GAPDH. *P<0.05 and **P<0.01 vs. the H_2O_2 group. Scale bar, 20 μm. NITyr, N-linoleyltyrosine; CB1 cannabinoid type 1; CB2 cannabinoid type 2.

stimulates an autophagic response, which in turn restores intracellular ROS levels. Decreased autophagy increases the accumulation of damaged organelles and ROS, which are involved in the pathogenesis of various diseases, including neurodegenerative conditions (28-30). According to the initial results of the present study, NITyr plays a considerable role in preventing H_2O_2-mediated cellular injury and ROS elevation, and therefore, the role of autophagy in these processes was investigated. When autophagy occurs, LC3 facilitates the formation of the autophagic membrane. A small segment of the cytoplasmic form of LC3 (LC3-I) is enzymatically degraded, and as such, LC3-I is transformed into membranous LC3 (LC3-II). The level of LC3-II, which is widely used to indicate overall autophagic degradation, has been significantly associated with the number of autophagosomes (31), and beclin-1 promotes the localization of autophagic proteins to autophagic vesicles (32). ATG13 is essential for autophagic vesicle formation (33), and ATG5 is a key regulator involved in the membrane extension of phagocytes into these vesicles (34). Thus, LC3, beclin-1, ATG5 and ATG13 play important roles in the formation and extension of autophagic vesicles. In the present study, NITyr was found to upregulate the protein expression levels of LC3-II, beclin-1, ATG5 and ATG13, indicating that it induces autophagy. To further elucidate the association between autophagy and oxidative stress, PC12 cells were treated with the autophagy inhibitor, 3MA, which was found to diminish the effects of NITyr on ROS generation and cellular viability. However, 3MA alone with H_2O_2 exposure did not affect cellular viability and the ROS levels. These results indicate that NITyr protects against cytotoxicity and excessive ROS production by activating autophagy.

AEA is an endogenous ligand of the cannabinoid receptor which has been reported to play an attenuative role in the pathogenesis and progression of neurodegenerative diseases (35). The CB1 receptor may be indirectly involved in oxidative stress (36). Conversely, the CB2 receptor is directly involved in counteracting oxidative stress (37). Additionally, AEA analogs have been associated with autophagy (9-11), and the protective functions of CB1 have also been linked to autophagy in various diseases (38). As an AEA analogue, NITyr may play a similar role to AEA. In the present study, PC12 cells were pre-treated with selective antagonists of the CB1 and CB2 receptors (AM251 and AM630, respectively), and AM251 pre-treatment blocked the protective effects of NITyr on H_2O_2-stimulated PC12 cells, while AM630 had no such effect. Moreover, AM251 and AM630 alone following H_2O_2 exposure did not affect cellular viability and the ROS levels. Therefore, the role of the CB1 receptor in NITyr-associated protection was the primary focus of the following experiments. Further experiments revealed that AM251 diminished the effects of NITyr on autophagy-related proteins, and confirmed that NITyr induced autophagy via the CB1 receptor, resulting in an antioxidant effect. Moreover, CB2 receptor expression in the presence of H_2O_2 remained the same as that under the control conditions, while the expression of the CB1 receptor was downregulated; these findings suggest that the CB2 receptor is highly stable, and that the CB1 receptor is more sensitive to oxidative stimuli. NITyr increased the expression of both the CB1 and CB2 receptor, whereas the CB2 receptor antagonist, AM630, was unable to inhibit the effects of NITyr. This may be due to the fact that the CB2 receptor is not highly expressed in PC12 cells, and that it is more prone to inflammatory stimulation, but not oxidative stress. It was further confirmed that the CB1 receptor may be the antioxidant target of NITyr.

To the best of our knowledge, the present study demonstrates for the first time that NITyr alleviates H_2O_2-induced injury and oxidative stress in PC12 cells by promoting autophagy. Furthermore, NITyr significantly maintained intracellular ROS homeostasis, reduced cellular injury and enhanced autophagy via the CB1 receptor. These findings suggest that NITyr inhibits oxidative stress through the CB1/ROS pathway with the involvement of autophagy. NITyr may therefore serve as a potential antioxidant by regulating the CB1 receptor.

Acknowledgements

Not applicable.

Funding

This study was supported by the National Natural Science Foundation of China (grant no. 81803514), the National Student Innovation Training Program (grant no. 202013705073), the Fund Project of Sichuan Provincial Department of Education (grant no. 18ZB0165), and the Fund Project of Development and Regeneration Key Laboratory of Sichuan Province (grant no. SYS15-007).

Availability of data and materials

The datasets used and/or analyzed during the current study are available from the corresponding author on reasonable request.

Authors' contributions

RY and SL designed and supervised the experiments. XL, YW and DZ performed the experiments, and YX and YL analyzed the data. YZ guided the immunofluorescence experiment, the data analysis and wrote the manuscript. SL provided approval of the final published version. All authors read and approved the final manuscript.

Ethics approval and consent to participate

Not applicable.

Patient consent for publication

Not applicable.

Competing interests

The authors declare that they have no competing interests.

References

1. Sies H: Oxidative stress: A concept in redox biology and medicine. Redox Biol 4: 180-183, 2015.
2. Tönnies E and Trushina E: Oxidative stress, synaptic dysfunction, and alzheimer's disease. J Alzheimers Dis 57: 1105-1121, 2017.
3. Salim S: Oxidative stress and the central nervous system. J Pharmacol Exp Ther 360: 201-205, 2017.
4. Ravanan P, Srikumar IF and Talwar P: Autophagy: The spotlight for cellular stress responses. Life Sci 188: 53-67, 2017.
5. De Munck D, De Meyer DR and Martinet W: Autophagy as an emerging therapeutic target for age-related vascular pathologies. Expert Opin Ther Targets 24: 131-145, 2020.
6. Filomeni G, De Zio D and Cecconi F: Oxidative stress and autophagy: The clash between damage and metabolic needs. Cell Death Differ 22: 377-388, 2015.
7. Fang C, Gu L, Smerin D, Mao S and Xiong X: Interrelation between reactive oxygen species and autophagy in neurological disorders. Oxi Med Cell Longev 2017: 8495160, 2017.
8. Martín Giménez VM, Noriega SE, Kassuha DE, Fuentes LB and Manucha W: Anandamide and endocannabinoid system: An attractive therapeutic approach for cardiovascular disease. Ther Adv Cardiovasc Dis 12: 177-190, 2018.
9. Hu Y, Tao Y and Hu J: Cannabinoid receptor 2 deletion deteriorates myocardial infarction through the down-regulation of AMPK-Mtor-p70S6K signaling-mediated autophagy. Biosci Rep 39: BSR20180650, 2019.
10. Wu A, Hu P, Lin J, Xia W and Zhang R: Activating cannabinoid receptor 2 protects against diabetic cardiomyopathy through autophagy induction. Front Pharmacol 9: 1292, 2018.
11. Wu Q, Zhang M, Liu X, Zhang J and Wang H: CB2R orchestrates neuronal autophagy through regulation of the mtor signaling pathway in the hippocampus of developing rats with status epilepticus. Int J Mol Med 45: 475-484, 2020.
12. Willoughby KA, Moore SF, Martin BR and Ellis EF: The biodisposition and metabolism of anandamide in mice. J Pharmacol Exp Ther 282: 243-247, 1997.
13. Cheng L, Li J, Zhou Y, Zheng Q, Ming X and Liu S: N-linoleyltyrosine protects against transient cerebral ischemia in gerbil via CB2 receptor involvement in PI3K/Akt signaling pathway. Biol Pharm Bull 42: 1867-1876, 2019.
14. Hu Y, Zhou KY, Wang ZJ, Lu Y and Yin M: N-stearoyl-l-tyrosine inhibits the cell senescence and apoptosis induced by H2O2 in HEK293/Tau cells via the CB2 receptor. Chem Biol Interact 272: 135-144, 2017.
15. Dyall SC, Mandhair HK, Fincham RE, Kerr DM, Roche M and Molina-Holgado F: Distinctive effects of eicosapentaenoic and docosahexaenoic acids in regulating neural stem cell fate are mediated via endocannabinoid signaling pathways. Neuropharmacology 107: 387-395, 2016.
16. Guo Z, Yuan Y, Guo Y, Wang H, Song C and Huang M: Nischarin attenuates apoptosis induced by oxidative stress in PC12 cells. Exp Ther Med 17: 663-670, 2019.
17. Maccarrone M: Metabolism of the endocannabinoid anandamide: Open questions after 25 years. Front Mol Neurosci 29: 166, 2017.
18. Zhang YB, Kan MY, Yang ZH, Ding WL, Yi J, Chen HZ and Lu Y: Neuroprotective effects of N-steroyltyrosine on transient global cerebral ischemia in gerbils. Brain Res 1287: 146-156, 2009.
19. Tang SQ, Yin S, Liu S, Le KJ, Yang RL, Liu JH, Wang XL, Zheng ZX, Zheng L, Lin Q and Lu Y: N-stearoyltyrosine dipotassium ameliorates high-fat diet-induced obesity in C57BL/6 mice. Eur J Pharm Sci 74: 18-26, 2015.
20. Liu S, Tang SQ, Cui HJ, Yin S, Yin M, Zhao H, Meng LH, Wang ZJ and Lu Y: Dipotassium N-stearoyltyrosinate ameliorated pathological injuries in triple-transgenic mouse model of alzheimer's disease. J Pharmacol Sci 132: 92-99, 2016.
21. Yao LY, Lin Q, Niu YY, Deng KM, Zhang JH and Lu Y: Synthesis of Lipoamino acids and their activity against cerebral ischemia injury. Molecules 14: 4051-4064, 2009.
22. Singh A, Kukreti R, Saso L and Kukreti S: Oxidative stress: A key modulator in neurodegenerative diseases. Molecules 22: 1583, 2019.
23. Chen L, Wu X, Shen T, Wang X, Wang S, Wang J and Ren D: Protective effects of ethyl gallate on H2O2-induced mitochondrial dysfunction in PC12 cells. Metab Brain Dis 34: 545-555, 2019.
24. Jia J, Ma L, Wu MC, Zhang L, Zhang X, Zhai Q, Jiang Q, Wang Q and Xiong L: Anandamide protects HT22 cells exposed to hydrogen peroxide by inhibiting cb1 receptor-mediated type 2 NADPH oxidase. Oxid Med Cell Longev 2014: 893516, 2014.
25. Wang ZH, Liu JL, Wu L, Yu Z and Yang HT: Concentration-dependent wrestling between detrimental and protective effects of H2O2 during myocardial ischemia/reperfusion. Cell Death Dis 5: e1297, 2014.
26. Martin D, Salinas M, Fujita N, Tsuruo T and Cuadrado A: Ceramide and reactive oxygen species generated by H2O2 induce caspase-3-independent degradation of Akt/protein kinase B. J Biol Chem 277: 42943-42952, 2002.

27. Denton D and Kumar S: Autophagy-dependent cell death. Cell Death Differ 26: 605-616, 2019.
28. Kaushal GP, Chandrashekar K and Juncos LA: Molecular interactions between reactive oxygen species and autophagy in kidney disease. Int J Mol Sci 20: 3791, 2019.
29. Wang H, Gao N, Li Z, Yang Z and Zhang T: Autophagy alleviates melamine-induced cell death in PC12 cells via decreasing ROS levels. Mol Neurobiol 53: 1718-1729, 2016.
30. Cao S, Li S, Li Q, Zhang F, Sun M, Wan Z and Wang S: Protective effects of salvianolic acid B against hydrogen peroxide-induced apoptosis of human umbilical vein endothelial cells and underlying mechanisms. Int J Mol Med 44: 457-468, 2020.
31. Cao Y, Chen J, Ren G, Zhang Y, Tan X and Yang L: Punicalagin prevents inflammation in LPS-induced RAW264.7 macrophages by inhibiting Fox3a/Autophagy signaling pathway. Nutrients 11: 2794, 2019.
32. Kang R, Zeh HJ, Lotze MT and Tang D: The beclin 1 network regulates autophagy and apoptosis. Cell Death Differ 18: 571-580, 2011.
33. Alers S, Wesselborg S and Stork B: ATG13: Just a companion, or an executor of the autophagic program? Autophagy 10: 944-956, 2014.
34. Arakawa S, Honda S, Yamaguchi H and Shimizu S: Molecular mechanisms and physiological roles of Atg5/Atg7-independent alternative autophagy. Proc Jpn Acad Ser B Phys Biol Sci 93: 378-385, 2017.
35. Moreira-Silva D, Carrettiero DC, Oliveira AS, Rodrigues S, Dos Santos-Lopes J, Canas PM, Cunha PA, Almeida MC and Ferreira TL: Anandamide effects in a streptozotocin-induced alzheimer's disease-like sporadic dementia in rats. Front Neurosci 12: 653, 2018.
36. Marsicano G, Moosmann B, Hermann H, Lutz B and Behl C: Neuroprotective properties of cannabinoids against oxidative stress: Role of the cannabinoid receptor CB1. J Neurochem 80: 448-456, 2002.
37. Parlar A, Arslan SQ, Doğan MF, Çam SA, Yalçin A, Elibol E, Özer MK, Üçkardeş F and Kara H: The exogenous administration of CB2 specific agonist, GW405833, inhibits inflammation by reducing cytokine production and oxidative stress. Exp Ther Med 16: 4900-4908, 2018.
38. Gugliandolo A, Pollastro F, Bramanti P and Mazzon E: Cannabidiol exerts protective effects in an in vitro model of parkinson's disease activating AKT/Mtor pathway. Fitoterapia 143: 104553, 2020.